

Effect of Voxel Size on the Accuracy of Landmark Identification in Cone-Beam Computed Tomography Images

Kyung-Min Lee¹, Kamran Davami², Hyeon-Shik Hwang¹, Byung-Cheol Kang³

¹Department of Orthodontics, School of Dentistry, Chonnam National University, ²School of Dentistry, Chonnam National University, ³Department of Oral and Maxillofacial Radiology, School of Dentistry, Chonnam National University, Gwangju, Korea

Purpose: This study was performed to evaluate the effect of voxel size on the accuracy of landmark identification in cone-beam computed tomography (CBCT) images.

Materials and Methods: CBCT images were obtained from 15 dry human skulls with two different voxel sizes; 0.39 mm and 0.10 mm. Three midline landmarks and eight bilateral landmarks were identified by 5 examiners and were recorded as three-dimensional coordinates. In order to compare the accuracy of landmark identification between large and small voxel size images, the difference between best estimate (average value of 5 examiners' measurements) and each examiner's value were calculated and compared between the two images.

Result: Landmark identification errors showed a high variability according to the landmarks in case of large voxel size images. The small voxel size images showed small errors in all landmarks. The landmark identification errors were smaller for all landmarks in the small voxel size images than in the large voxel size images.


Conclusion: The results of the present study indicate that landmark identification errors could be reduced by using smaller voxel size scan in CBCT images.

Key Words: Cone-beam computed tomography; Orthodontics

Introduction

Cone-beam computed tomography (CBCT) has been widely used in orthodontics since its introduc-

tion in dentistry in 1998¹). Applications of CBCT images in orthodontics include dental measurements²), evaluation of root resorption³), diagnoses of the temporomandibular joint^{4,5}), airway assessment⁶), three-

Corresponding Author: **Byung-Cheol Kang**,  <https://orcid.org/0000-0003-1944-5985>

Department of Oral and Maxillofacial Radiology, School of Dentistry, Chonnam National University, 33 Yongbong-ro, Buk-gu, Gwangju 61186, Korea

TEL : +82-62-530-5686, FAX : +82-62-530-5659, E-mail : bckang@jnu.ac.kr

Received for publication February 22, 2019; Returned after revision May 30, 2019; Accepted for publication June 24, 2019

Copyright © 2019 by Korean Academy of Dental Science

 This is an open access article distributed under the terms of the Creative Commons Attribution Non-Commercial License (<http://creativecommons.org/licenses/by-nc/4.0>) which permits unrestricted non-commercial use, distribution, and reproduction in any medium, provided the original work is properly cited.

dimensional (3D) cephalometry⁷⁾, and evaluation of orthognathic surgery⁸⁾.

The image quality of CBCT scan might be influenced by a number of variables, such as the scanning unit, the field of view (FOV), subject characteristics, scanning time, tube voltage and tube current, and also spatial resolution defined by the voxel size⁹⁻¹¹⁾. CBCT volumetric data set is composed of volume elements called voxels and the dimension of each voxel determines spatial resolution of the image¹²⁾. Images acquired in smaller voxel sizes or smaller FOV have better spatial resolution. Maret et al.¹⁰⁾ assessed the effect of voxel size on the accuracy of 3D reconstruction of CBCT data. They found that volumetric measurements at voxel size of 200 μm and 300 μm were underestimated by comparing with those obtained with voxel size of 76 μm and 41 μm . In contrast, Damstra et al.¹³⁾ suggested that there was no statistically significant difference of the linear measurement accuracy between 0.40 mm and 0.25 mm voxel size group.

Landmark-based analysis of maxillofacial structure with linear and angular measurements is the most common method of cephalometric analysis in orthodontics since Broadbent¹⁴⁾ introduced cephalometric radiography. However, in the literature, few studies so far have assessed the effect of voxel size on the accuracy of landmark identification in the CBCT images. The purpose of the present study was to investigate the effect of voxel size on the accuracy of landmark identification in CBCT images.

Materials and Methods

The present study was approved by the Institutional Review Board (IRB) of Chonnam National

University Dental Hospital (IRB No. CNUDH-EXP-2015-001). A total of fifteen dry human skulls from Department of Oral Anatomy at the School of Dentistry of Chonnam National University were included in this study. The skulls were placed in the acrylic box and stabilized with sticks on both ear holes and occipital area. The condyle for each skull was isolated from temporal fossa by a paper with 1.5 mm thickness to define the exact contours of condyle.

CBCT scans were obtained with Alphard VegaTM (Asahi Roentgen Co., Kyoto, Japan) in two different voxel sizes: 0.39 mm and 0.10 mm. The scans for both voxel sizes were taken with 80 kV for voltage and 17 seconds for exposure time. Tube current and FOV for voxel size of 0.39 mm were 5 mA and 200×179 mm and those for voxel size of 0.10 mm were 8 mA and 51×51 mm, respectively (Table 1).

Seven CBCT scans for each skull were obtained in same head posture. One CBCT scan of whole skull with large voxel size and 6 CBCT scans with small voxel size were obtained from each skull. For small voxel size scan, 6 areas (condyle, frontonasal, gonion, orbit, symphysis, and nasomaxillary areas) were included. In case of bilateral structures such as condyle, gonion, and orbit, right side area was scanned (Fig. 1).

CBCT scan data were exported to InVivoDentalTM software ver. 5.1 (Anatomage, San Jose, CA, USA) as a digital imaging and communication in medicine (DICOM) file. Using 'volume rendering' function of the software, 3D surface model was visualized in 'bone' mode. The minimum and maximum thresholds were 620 and 3,640 gray scale values, respectively.

To investigate the effect of voxel size on the ac-

Table 1. Scanning parameters for large and small voxel size scans used in this study

Variable	Voxel size (mm)	Field of view (mm)	Voltage (kV)	Current (mA)	Exposure time (s)
Large	0.39	200×179	80	5	17
Small	0.10	51×51	80	8	17

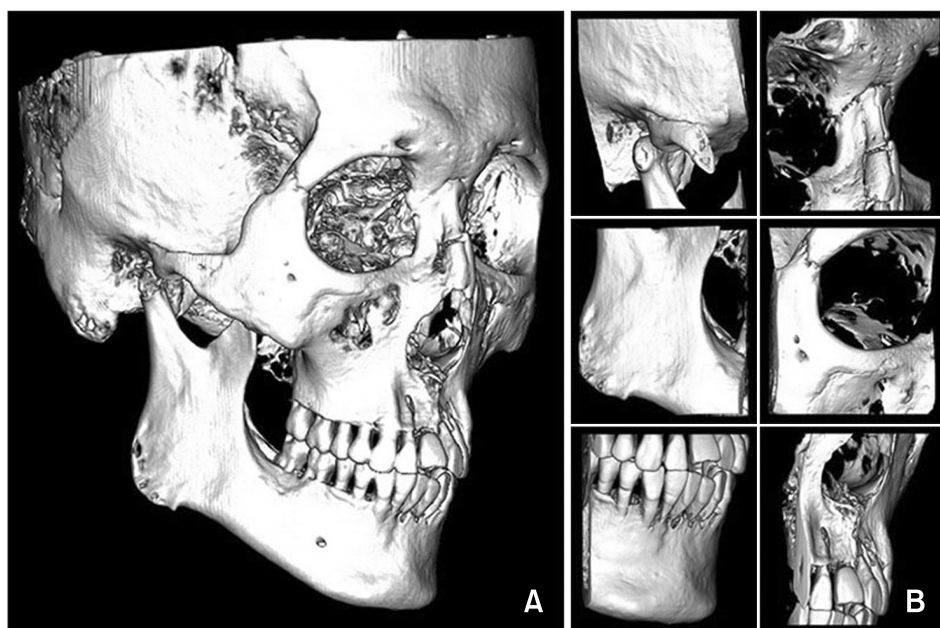


Fig. 1. Two different voxel size images obtained in this study. (A) 0.39 mm voxel size image; (B) 0.10 mm voxel size images.

Table 2. Definition of the landmarks used in this study

Landmark	Abbreviation	Definition
Midline landmark		
Crista galli	Cg	Most superior point of cista galli of ethmoid bone
Anterior nasal spine	ANS	Most anterior midpoint of the anterior nasal spine
Menton	Me	Most inferior point on mandibular symphysis
Bilateral landmark		
Orbitale	Or	Deepest point on infraorbital margin
Porion	Po	Highest point on roof of external auditory meatus
Condylion superius	Cd _{sup}	Most superior point of each mandibular condylar head
Condylion lateralis	Cd _{lat}	Most lateral point of each mandibular condylar head
Condylion posterius	Cd _{post}	Most posterior point of each mandibular condylar head
Gonion lateralis	Go _{lat}	Most lateral point on gonion area
Gonion posterius	Go _{post}	Most posterior point on gonion area
Gonion inferius	Go _{inf}	Most inferior point on gonion area

curacy of landmark identification in CBCT surface model, three midline landmarks (crista galli, anterior nasal spine, and menton) and eight bilateral landmarks (orbitale, porion, condylion superius, condylion lateralis, condylion posterius, gonion lateralis, gonion posterius, and gonion inferius) were used in this study¹⁵. The landmarks were identified by 5 examiners experienced in landmark identification on 3D surface model with over 50 cases (Table 2). The examiners were permitted to rotate the image to

improve landmark visibility. Both large and small voxel size scans had same spatial orientation of the acquired volume. For each of the 11 landmarks, the mean x-, y-, and z-coordinates from all 5 examiners were defined as the best estimate. The landmark identification error was defined as a measurement in millimeters by calculating the distance of each examiner's identification from the best estimate¹⁶. In addition, their mediolateral, anteroposterior, and infero-superior components were expressed by calculating

differences in the x-, y-, and z-coordinates from those of the best estimates (Table 2).

Paired t-tests were used to determine differences between the large and small voxel size images. In addition, the means and standard deviations were computed for each coordinate direction in order to evaluate which direction of the error contributed to the degree of overall error. Paired t-tests were used to determine the differences of the errors in 3D between the large and small voxel size images. Statistical analysis was carried out by using PASW software ver. 18.0 (IBM Corp., Armonk, NY, USA) ($P < 0.05$).

Result

The landmark identification errors showed variability according to the landmark. In the case of the large voxel size images, the errors ranged from 0.57 to 1.94 mm. All midline landmarks and orbitale showed relatively small errors compared to the bilateral landmarks (porion, condylion, and gonion). In particular, porion presented the greatest error of 1.94 mm. On the other hand, the identification errors in small voxel size images showed below 0.6 mm in all

landmarks except porion which presented 0.92 mm of error. In the comparison of identification error, all landmarks except for orbitale showed statistically significant differences between the two sizes indicating that the errors could be reduced by using small voxel size scan (Table 3).

In order to evaluate which direction of error contributed to the degree of overall error, the means and standard deviations were computed for each coordinate direction. In case of porion which showed largest value (1.94 mm) in overall error, the x-direction error (1.59 mm) was greater compared to the y- or z-direction errors indicating that large identification errors in porion were attributed mostly to the mediolateral direction error. Likewise, condylion superius also showed a greater value in the x-direction errors. With regards to gonion, gonion lateralis and gonion inferius showed relatively large values in the y-direction errors (0.87 and 0.82 mm, respectively) whereas gonion posterius presented a relatively large error in the z-direction (0.69 mm). While the errors were considerably greater in the large voxel size images, all these errors showed small values in the small voxel size images. The differences between

Table 3. Landmark identification errors and comparison between large and small voxel size images

	Large voxel size (mm)	Small voxel size (mm)	Difference (large to small, mm)	Significance (P-value)
Midline landmark				
Crista galli	0.67±0.68	0.20±0.18	0.47	<0.001
Anterior nasal spine	0.80±0.60	0.40±0.46	0.40	<0.001
Menton	0.71±0.49	0.41±0.32	0.30	<0.001
Bilateral landmark				
Orbitale	0.57±0.35	0.38±0.32	0.19	0.001
Porion	1.94±1.92	0.92±0.75	1.02	<0.001
Condylion superius	1.34±1.20	0.53±0.40	0.81	<0.001
Condylion lateralis	1.31±1.66	0.31±0.34	1.00	<0.001
Condylion posterius	0.97±0.65	0.57±0.62	0.40	<0.001
Gonion lateralis	1.24±1.33	0.54±0.45	0.70	<0.001
Gonion posterius	0.90±0.63	0.43±0.35	0.47	<0.001
Gonion inferius	1.09±0.90	0.37±0.28	0.73	<0.001

Values are presented as mean±standard deviation.

the large and small voxel size images were statistically significant in all directions of all landmarks except the y-direction error in orbitale which showed

small value even in the large voxel size images and z-direction error in porion which showed relatively large value even in small voxel size images (Table 4).

Table 4. Landmark identification errors in 3-dimension and comparison between large and small voxel size

	Large voxel size (mm)	Small voxel size (mm)	Difference (large to small, mm)	Significance (P-value)
X-direction errors				
Crista galli	0.16±0.15	0.07±0.16	0.09	0.002
Anterior nasal spine	0.37±0.36	0.25±0.36	0.11	0.013
Menton	0.31±0.30	0.20±0.28	0.11	<0.001
Orbitale	0.43±0.37	0.26±0.28	0.17	0.002
Porion	1.59±1.93	0.59±0.66	1.00	0.001
Condylion superius	0.97±1.06	0.39±0.41	0.58	<0.001
Condylion lateralis	0.64±1.67	0.09±0.20	0.55	0.006
Condylion posterius	0.67±0.58	0.40±0.07	0.27	0.002
Gonion lateralis	0.32±0.58	0.08±0.10	0.24	0.001
Gonion posterius	0.37±0.31	0.17±0.14	0.20	<0.001
Gonion inferius	0.46±0.38	0.17±0.15	0.29	<0.001
Y-direction errors				
Crista galli	0.46±0.55	0.13±0.12	0.33	<0.001
Anterior nasal spine	0.51±0.57	0.16±0.31	0.34	<0.001
Menton	0.55±0.46	0.28±0.21	0.27	<0.001
Orbitale	0.21±0.17	0.20±0.20	0.01	NS
Porion	0.69±0.69	0.39±0.40	0.30	<0.001
Condylion superius	0.41±0.38	0.21±0.23	0.20	0.009
Condylion lateralis	0.56±0.56	0.14±0.13	0.41	<0.001
Condylion posterius	0.24±0.20	0.13±0.17	0.11	<0.001
Gonion lateralis	0.87±1.02	0.46±0.45	0.41	0.001
Gonion posterius	0.22±0.23	0.09±0.10	0.13	<0.001
Gonion inferius	0.82±0.87	0.27±0.28	0.55	<0.001
Z-direction errors				
Crista galli	0.32±0.48	0.07±0.06	0.26	<0.001
Anterior nasal spine	0.30±0.26	0.13±0.18	0.18	<0.001
Menton	0.16±0.12	0.12±0.12	0.06	0.001
Orbitale	0.18±0.13	0.11±0.09	0.06	<0.001
Porion	0.35±0.34	0.32±0.45	0.03	NS
Condylion superius	0.51±0.09	0.12±0.01	0.39	<0.001
Condylion lateralis	0.60±0.53	0.21±0.29	0.39	<0.001
Condylion posterius	0.49±0.47	0.28±0.26	0.22	<0.001
Gonion lateralis	0.55±0.88	0.12±0.18	0.36	0.001
Gonion posterius	0.69±0.64	0.34±0.35	0.37	<0.001
Gonion inferius	0.28±0.37	0.07±0.06	0.21	<0.001

NS: statistically not significant.

Values are presented as mean±standard deviation.

Discussion

For orthodontic purpose, large FOV images are preferred for the evaluation of the craniomaxillofacial images. However, large FOV images have lower resolution and higher patient radiation dose. To reduce the patients' radiation exposure, it is desirable to limit the field size to the smallest volume that visualizes only the region of interest. Decrease in voxel size may exhibit advantages, such as higher quality of images, more accurate anatomic details, and smaller radiation exposure, and also disadvantages such as more noises in the image. Detectors with smaller pixels capture fewer X-ray photons per voxel and result in more image noise¹⁷⁾.

The average coordinates of all the examiners for each landmark in two different voxel size served as the best estimate for that particular landmark in this study. The distances from this best estimate were used as the landmark identification error for each landmark in two different voxel sizes. Schlicher et al.¹⁶⁾ provided the mean location for each landmark as the reference point and assessed the distribution of examiners' landmarks from this point to quantify the consistency and precision of locating 3D anatomic landmarks. In the study of Leonardi et al.¹⁸⁾, the mean positions for each landmark identified by the five observers were defined as the best estimate for that particular landmark in a given two-dimensional (2D) image. As the best estimate from all the examiners was used as the gold standard, our eligibility criteria for the examiner of this study was orthodontic residents who had experienced in landmark identification on 3D surface model with over 50 cases.

Although one cannot expect higher accuracy than in the range of half a millimeter on dental CBCT images¹⁹⁾, the mean values of the landmark identification errors ranged from 0.57 to 1.94 mm in large voxel size images and 0.20 to 0.92 mm in small voxel size images in this study indicating that there was variability of landmark identification. While all mid-

line landmarks and orbitale presented small values of the errors, the other bilateral landmarks (porion, condyle, and gonion) showed large errors.

Small voxel size images showed statistically significant smaller errors than large voxel size images. It could be contributed to the clearer images with less artifacts and more anatomic details in small voxel size scans that would increase the accuracy of landmark identification. In case of small voxel size images, the image display for the reorientation in three planes (sagittal, coronal, and axial) were not available due to the small FOV. In other words, landmark identification in small voxel size images might be influenced by inconsistency in the image orientation of the small FOV scan. However, in the present study, both large and small voxel size scans had same spatial orientation of the acquired volume and the landmark identification errors in small voxel size images showed small value compared to the large voxel size images, implying no remarkable influence by the image orientation.

In case of large voxel size images, identification errors were smaller in midline landmarks and orbitale than bilateral landmarks. Schlicher et al.¹⁶⁾ claimed that midline structures and their landmarks formed by acute angles were more consistently identified than bilateral structures and their landmarks along broad curves. Thus it is believed that the midline landmarks inherently cause minimal errors in the x-coordinates.

The largest identification errors of porion in both large and small voxel size images were attributed to x-direction of errors. Once the examiner identified porion on the highest point on roof of external auditory meatus, it may refer to multiple points in mediolateral direction and thus increase the x-direction errors. Likewise, condylion superius also showed large error in the x-direction. gonion, gonion lateralis and gonion inferius showed greater y-direction errors whereas gonion posterius presented greater z-direction errors than in the other coordinates. This

finding should be taken into consideration that the landmark with the smallest error should be selected when constructing the measurement by connecting the two landmarks.

The y-direction error in orbitale was relatively small even in the large voxel size images and the z-direction error in porion was relatively large even in small voxel size images. Anatomical position of the landmarks may have contributed to the results, *i.e.*, exact definition of orbitale location in y-direction could decrease the identification error even in large voxel size images. Likewise, porion lacks of definition of exact location in the sagittal direction and could cause large identification errors in the z-direction even in small voxel size images. Another possible reason is anatomic position of porion; round beveled curve of the roof of external auditory meatus may increase the error not only in the z-direction but in the x and y-direction as well even in small voxel size images. In spite of the significant landmark identification error, some have used porion for the construction of reference planes for evaluation of facial asymmetry²⁰⁻²⁴⁾. Considering the reliability of the landmark identification and the potential errors in defining the reference planes, it can be suggested to use other non-anatomic structures to construct the references planes for measurement accuracy²⁵⁾. Additionally, in a recent study²⁶⁾, the inter-examiner errors in 2D posteroanterior cephalometric radiographs were reported as 0.6 mm to 2.5 mm. Taken together, the errors in the present study might be clinically acceptable.

Although small voxel size images showed smaller errors than large ones, CBCT scans with small voxel size may not be readily recommended as the routine imaging protocol in orthodontics because small FOV images require a number of scans which increase patient's radiation exposure. Nonetheless, the results of the present study can help understanding characteristics of the 3D landmark identification errors and improving the measurement accuracy. Recently,

current development of imaging sensor technology may make voxel size as small as 0.1 mm, while minimizing radiation exposure. Alternatively, acquisition of small voxel size images for the area of clinical significance and merging them with the background large voxel size image(s) may be recommended.

Conclusion

1. Landmark identification errors showed relatively higher variability in case of large voxel images compare to those of small voxel size.
2. The landmark identification errors could be reduced by using smaller voxel size scan in CBCT images.

Conflict of Interest

No potential conflict of interest relevant to this article was reported.

References

1. Mozzo P, Procacci C, Tacconi A, Martini PT, Andreis IA. A new volumetric CT machine for dental imaging based on the cone-beam technique: preliminary results. *Eur Radiol.* 1998; 8: 1558-64.
2. Baumgaertel S, Palomo JM, Palomo L, Hans MG. Reliability and accuracy of cone-beam computed tomography dental measurements. *Am J Orthod Dentofacial Orthop.* 2009; 136: 19-25; discussion 25-8.
3. Dudic A, Giannopoulou C, Leuzinger M, Kiliaridis S. Detection of apical root resorption after orthodontic treatment by using panoramic radiography and cone-beam computed tomography of super-high resolution. *Am J Orthod Dentofacial Orthop.* 2009; 135: 434-7.
4. Honey OB, Scarfe WC, Hilgers MJ, Klueber K, Silveira AM, Haskell BS, Farman AG. Accuracy of cone-beam computed tomography imaging of

- the temporomandibular joint: comparisons with panoramic radiology and linear tomography. *Am J Orthod Dentofacial Orthop.* 2007; 132: 429-38.
5. Barghan S, Merrill R, Tetradis S. Cone beam computed tomography imaging in the evaluation of the temporomandibular joint. *J Calif Dent Assoc.* 2010; 38: 33-9.
 6. Aboudara C, Nielsen I, Huang JC, Maki K, Miller AJ, Hatcher D. Comparison of airway space with conventional lateral headfilms and 3-dimensional reconstruction from cone-beam computed tomography. *Am J Orthod Dentofacial Orthop.* 2009; 135: 468-79.
 7. Wong RW, Chau AC, Hägg U. 3D CBCT McNamara's cephalometric analysis in an adult southern Chinese population. *Int J Oral Maxillofac Surg.* 2011; 40: 920-5.
 8. Cevidanes LH, Bailey LJ, Tucker SF, Styner MA, Mol A, Phillips CL, Proffit WR, Turvey T. Three-dimensional cone-beam computed tomography for assessment of mandibular changes after orthognathic surgery. *Am J Orthod Dentofacial Orthop.* 2007; 131: 44-50.
 9. Scarfe WC, Farman AG. What is cone-beam CT and how does it work? *Dent Clin North Am.* 2008; 52: 707-30, v.
 10. Maret D, Telmon N, Peters OA, Lepage B, Treil J, Inglès JM, Peyre A, Kahn JL, Sixou M. Effect of voxel size on the accuracy of 3D reconstructions with cone beam CT. *Dentomaxillofac Radiol.* 2012; 41: 649-55.
 11. Donaldson K, O'Connor S, Heath N. Dental cone beam CT image quality possibly reduced by patient movement. *Dentomaxillofac Radiol.* 2013; 42: 91866873.
 12. Hatcher DC. Operational principles for cone-beam computed tomography. *J Am Dent Assoc.* 2010; 141(Suppl 3): 3S-6S.
 13. Damstra J, Fourie Z, Huddleston Slater JJ, Ren Y. Accuracy of linear measurements from cone-beam computed tomography-derived surface models of different voxel sizes. *Am J Orthod Dentofacial Orthop.* 2010; 137: 16.e1-6; discussion 16-7.
 14. Broadbent BH. A new X-ray technique and its application to orthodontia. *Angle Orthod* 1931; 1: 45-66.
 15. Hwang HS, Hwang CH, Lee KH, Kang BC. Maxillofacial 3-dimensional image analysis for the diagnosis of facial asymmetry. *Am J Orthod Dentofacial Orthop.* 2006; 130: 779-85.
 16. Schlicher W, Nielsen I, Huang JC, Maki K, Hatcher DC, Miller AJ. Consistency and precision of landmark identification in three-dimensional cone beam computed tomography scans. *Eur J Orthod.* 2012; 34: 263-75.
 17. Scarfe WC, Farman AG. Cone-beam computed tomography: volume acquisition. In: Mallya S, Lam E, eds. *White and pharaoh's oral radiology: principles and interpretation.* St. Louis, MO: Elsevier; 2019. p. 151-64.
 18. Leonardi RM, Giordano D, Maiorana F, Greco M. Accuracy of cephalometric landmarks on monitor-displayed radiographs with and without image emboss enhancement. *Eur J Orthod.* 2010; 32: 242-7.
 19. Brüllmann D, Schulze RK. Spatial resolution in CBCT machines for dental/maxillofacial applications-what do we know today? *Dentomaxillofac Radiol.* 2015; 44: 20140204.
 20. Park SH, Yu HS, Kim KD, Lee KJ, Baik HS. A proposal for a new analysis of craniofacial morphology by 3-dimensional computed tomography. *Am J Orthod Dentofacial Orthop.* 2006; 129: 600.e23-34.
 21. Maeda M, Katsumata A, Arijii Y, Muramatsu A, Yoshida K, Goto S, Kurita K, Arijii E. 3D-CT evaluation of facial asymmetry in patients with maxillofacial deformities. *Oral Surg Oral Med Oral Pathol Oral Radiol Endod.* 2006; 102: 382-90.
 22. Terajima M, Nakasima A, Aoki Y, Goto TK, Tokumori K, Mori N, Hoshino Y. A 3-dimensional method for analyzing the morphology of patients with maxillofacial deformities. *Am J Orthod Dentofacial Orthop.* 2009; 136: 857-67.
 23. Damstra J, Oosterkamp BC, Jansma J, Ren Y. Combined 3-dimensional and mirror-image analysis for

- the diagnosis of asymmetry. *Am J Orthod Dentofacial Orthop.* 2011; 140: 886-94.
24. Kim SJ, Lee KJ, Lee SH, Baik HS. Morphologic relationship between the cranial base and the mandible in patients with facial asymmetry and mandibular prognathism. *Am J Orthod Dentofacial Orthop.* 2013; 144: 330-40.
25. Hwang HS, Lee KM, Uhm GS, Cho JH, McNamara JA Jr. Use of Reference Ear Plug to improve accuracy of lateral cephalograms generated from cone-beam computed tomography scans. *Korean J Orthod.* 2013; 43: 54-61.
26. Hwang SA, Lee JS, Hwang HS, Lee KM. Benefits of lateral cephalogram during landmark identification on posteroanterior cephalograms. *Korean J Orthod.* 2019; 49: 32-40.